JOURNAL OF MATERIALS SCIENCE 25 (1990) 3475–3483

Microstructure and superconducting current of *in situ* Nb_3Sn superconducting wire

SHOJIRO OCHIAI, KOZO OSAMURA, TAKATO KITAI, YUICHI YAMADA
Department of Metallurgy, Kyoto University, Sakyo-ku, Kyoto 606, Japan

The diffusion of elemental tin and the morphological change of niobium filaments in *in situ* Nb_3Sn superconducting composite wires and their influences on critical current were studied. When the amount of tin plated on the samples was high, the diffusion of elemental tin was enhanced. The critical current increased with increasing tin concentration but the increase became sluggish at high tin contents. The niobium filaments were initially ribbon-like but they became rod-like and then sausage-like after annealing treatment. Such a morphological change acted to reduce superconducting current capacity. When the amount of niobium was low, the filaments spheroidized by high-temperature and long-term annealing, resulting in serious reduction in critical current and upper critical magnetic field. High niobium contents led to high critical current and high upper critical magnetic field due to retainment of continuity of the filaments after annealing, effective proximity effect and a high amount of Nb_3Sn formed in comparison with low niobium content amount. The titanium addition raised the upper critical magnetic field, resulting in improvement in critical current at high magnetic fields.

1. Introduction

The *in situ* Nb_3Sn superconductors have advantages in comparison to the conventional bronze-processed ones in that they (a) can be prepared by a simple and economical processing method [1], (b) have high mechanical properties [2, 3], (c) have high critical current density [4], (d) have high strain tolerance [5, 6], and (e) can be prepared at a relatively low heat-treatment temperature [1].

In the *in situ* prepared Nb_3Sn superconductors, the critical current has a strong correlation to the microstructure as in conventionally prepared superconductors. The microstructure is affected by the size of the samples, the amount and morphology of niobium filaments, the thickness of the copper cladding, and the addition of third elements [7]. However, there are two big differences between conventional and *in situ* methods: (1) tin is supplied from the bronze matrix in the conventional method while it is supplied from an internal or external tin layer in the *in situ* method, resulting in inhomogeneous tin concentration on a macro-scale in the latter method, and (2) niobium filaments are very fine in the *in situ* method, resulting in coarsening during heat-treatment. Such differences between the two methods lead to different microstructure, which affects the critical current. In the *in situ* samples, the correlation between the microstructure and superconducting current has, however, not necessarily been clarified.

In the present work, tin was plated on to the samples, and the microstructural change of the *in situ* prepared samples due to heat treatment and its influence on critical current, were studied.

2. Experimental procedure

Samples without tin plating were supplied as the Japanese Standard Reference Sample for the superconducting materials group for energy research of the Ministry of Education, Science and Culture of Japan. The specifications of the as-supplied samples are listed in Table I.

The as-supplied samples were cut to 40 mm length and plated electrically with tin. Some as-supplied samples were plated with various amounts of tin in order to study the influence of tin thickness on superconducting properties. The results showed that higher amounts lead to higher superconducting properties, as shown later. On the other hand, when the tin layer became too great, the samples became very fragile, resulting in a difficulty of handling. Most samples were therefore plated with the amount indicated in Table II in which the figures shown in the parentheses correspond to the amounts necessary to convert all niobium to Nb_3Sn. The samples were heat-treated in vacuum first at 483 K for 432 ksec in order to form intermetallic compounds with high melting points.

TABLE I Specification of the samples employed in the present work

Wire diameter	0.3 mm
Composition	Cu–10, 20, 25, 30, 40 wt % Nb Cu–25 wt % Nb–0.5 wt % Ti
Thickness of copper cladding	18 μm
Area-reduction ratio	4×10^4

0022–2461/90 $03.00 + .12

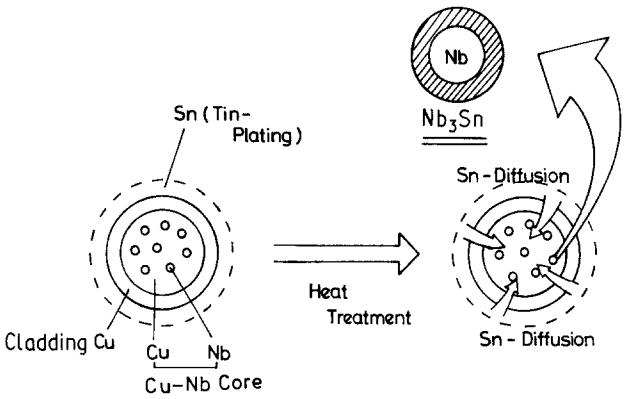

Figure 1 Schematic representation of an external diffusion method for *in situ* composite wire.

Otherwise, the plated tin melts upon heating, flowing down from the samples. After this pre-annealing treatment, the samples were annealed at 823 and 973 K for up to 2000 ksec. The pre-annealing treatment was common for all samples. Hereafter, unless noted, the final annealing treatment is termed simply the annealing treatment.

The morphology of the niobium filaments was observed by SEM after etching away the matrix. The diffusion of elemental tin was measured by electron probe microanalysis (EPMA).

The critical current was measured at 4.2 K in the magnetic field, H, from 2 to 15 T by a 1 $\mu V cm^{-1}$ criterion for critical current using the WM-5 magnet of the High Field Laboratory for Superconducting Materials, Tohoku University.

3. Results and discussion

3.1. Diffusion of elemental tin

3.1.1. Influence of amount of tin on diffusion profile and superconducting properties

The tin plated on the copper cladding diffuses first into the cladding and then into the inner Cu–Nb core where niobium filaments exist. When tin reaches the core, it reacts with niobium filaments to form Nb_3Sn, as shown schematically in Fig. 1. As a result, the absorption images and distribution of the elemental tin vary with annealing temperature and time as typically shown in Fig. 2 in which the samples with 40 wt % Nb annealed at (a) 823 K for 1000 ksec and (b) 973 K for 432 ksec are presented as examples. The tin concentration was high in the dark region and very low (nearly the noise level) in the bright region in the absorption images. When tin reached the centre of the core, the bright region disappeared.

TABLE II Amount of plated tin. The figures in parentheses show the amounts of tin necessary to convert all niobium to Nb_3Sn.

Composition of samples	Amount of plated tin (wt %)
Cu–10 wt % Nb	6(3.2)
Cu–25 wt % Nb	12(7.9)
Cu–25 wt % Nb–0.5 wt % Ti	12(7.9)
Cu–40 wt % Nb	18(12.7)

First, in order to determine the influence of the amount of plated tin on the diffusion of tin and the superconducting properties, various amounts of tin were plated on 25 wt % Nb samples and then annealed by the procedure given in Section 2. Fig. 3 shows the tin profiles for 2, 6 and 10 wt % Sn plating, followed by annealing at 823 K for (a) 500 and (b) 1500 ksec. The following features can be seen in Fig. 3. (1) High tin amounts enhanced the diffusion of elemental tin. (2) The tin concentration in the region where it had diffused was high in the high tin content samples, suggesting high amounts of formation of Nb_3Sn in these samples. (3) As expected, when the tin content was low, elemental tin could not reach the centre of the Cu–Nb core, even after long annealing times.

Fig. 4 shows the variations of (a) critical current density, J_c, based on the cross-sectional area of the Cu–Nb core at an applied magnetic field of H = 5, 9 and 12 T, and (b) the upper critical magnetic field, H_{c2}, inferred from the Kramer plot [8, 9] as a function of tin content. J_c and H_{c2} increased with increasing tin content but the increase became sluggish around 8%.

Two possible explanations may be put forward for the increase in J_c and H_{c2} for high tin contents. (i) As stated above, the amount of Nb_3Sn formed was high when the tin content was high. (ii) It has been reported that, in the conventional bronze-processed Nb_3Sn

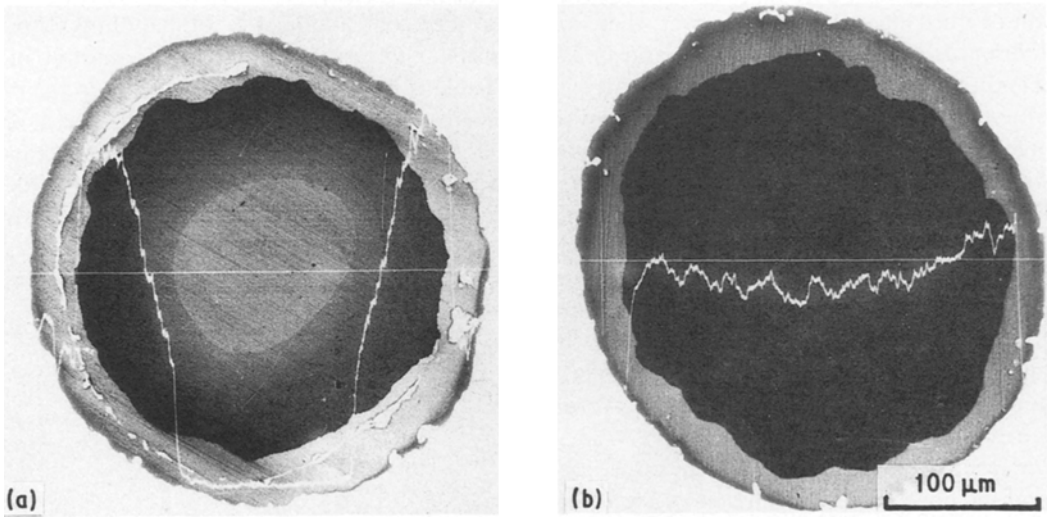

Figure 2 Absorption images and distribution of elemental tin in the Cu–40 wt % Nb samples annealed at (a) 823 K for 1000 ksec, and (b) 973 K for 432 ksec.

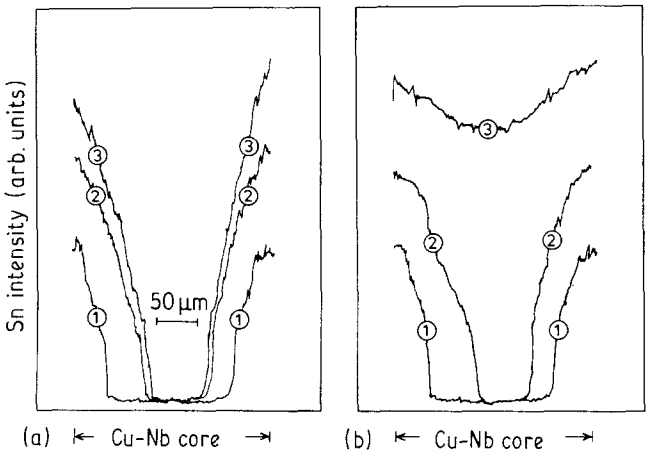

Figure 3 Distribution of elemental tin measured with EPMA in the Cu–25 wt % Nb samples plated with (1) 2, (2) 6 and (3) 10 wt % tin and annealed at 823 K for (a) 500 and (b) 1500 ksec.

superconductors, the Nb_3Sn formed in the high tin bronze matrix has superior superconducting properties to that in the low tin bronze matrix [9]. The same mechanism seems to arise in the present samples.

From the experimental results stated above, it was demonstrated that high tin contents lead to high superconducting properties. In the 25 wt % Nb samples, the amount of tin necessary to convert all niobium to Nb_3Sn was calculated to be 7.9 wt %. The amount of 7.9% was, however, insufficient to achieve high superconducting properties, partly because copper can contain elemental tin, which was not taken into consideration in the calculation. Although high tin contents lead to high superconducting properties, it also makes the samples very fragile, which gives difficulty in handling. In the following study, the amount of tin used was therefore as high as possible within the range of easy handling. The amount of tin plated in the study is shown in Table II in which the amount of tin necessary to convert all niobium to Nb_3Sn is shown in parentheses for comparison.

3.1.2. *Influence of annealing time, content of niobium filaments and addition of titanium on diffusion of elemental tin*

Typical tin profiles in the annealed samples are presented in Fig. 5, whose profiles were measured under the same operating condition to make comparison with each other possible. With increasing annealing time, the diffusion front approached the centre of the Cu–Nb core and reached it for long annealing times, as shown in Fig. 5a. The tin concentration in the region where the diffusion front had passed increased with increasing time, suggesting an increase in the amount of Nb_3Sn in this region. The tin diffused faster in the samples containing low niobium contents than in the samples containing high amounts, as shown in Fig. 5b. One reason for this is that the niobium filaments act as a barrier to the diffusion of tin, and another is that more tin is consumed for formation of Nb_3Sn in the samples containing more niobium filaments. The diffusion rate of tin was not influenced so much by the titanium addition, as shown in Fig. 5c. However, it should be noted that, on addition of titanium the tin concentration became higher in the region where tin had diffused. This might be attributed to the enhancement of the growth rate of the Nb_3Sn by the addition of titanium as has been observed in conventional bronze-processed Nb_3Sn superconductors with titanium addition [9–13].

The cross-sectional area, S, of the region in which tin had diffused, corresponding to the dark region shown in Fig. 2, was measured. The results are shown in Fig. 6 . With increasing of niobium content, the time necessary for elemental tin to reach the centre increased.

3.2. Coarsening of filaments

The shape of the niobium filaments in the as-supplied samples was ribbon-like, as shown in Fig. 7a. The thickness was about 20 nm and the width about 200 nm. The filaments showed a dramatic change in shape and size when the samples were annealed. Typical examples are shown in Figs 7b to d in which the morphologies of the filaments, composed of Nb_3Sn and unreacted niobium, in 25 wt % Nb samples annealed at 773, 873 and 1073 K for 864 ksec are presented, respectively. When annealed, the filaments

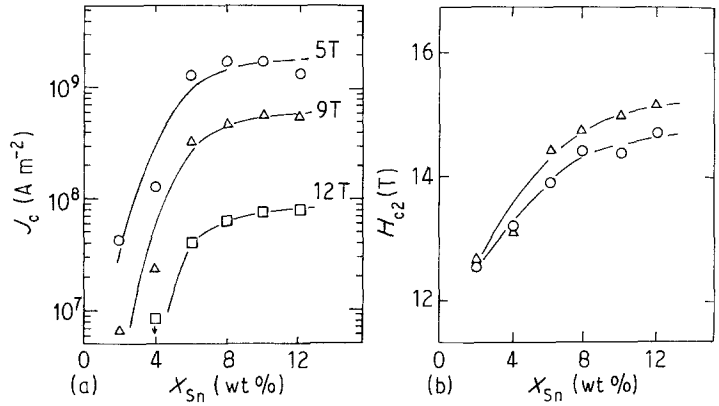

Figure 4 Influence of tin content, X_{Sn}, on (a) J_c and (b) H_{c2} of the Cu–25 wt % Nb samples. (a) 1500 k sec, (b) (○) 500 ksec, (△) 1500 ksec.

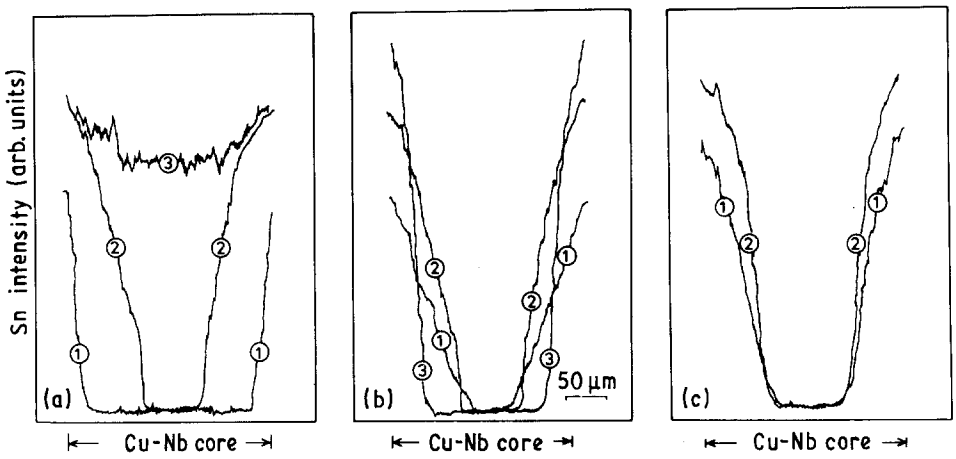

Figure 5 Influence of (a) annealing time, (b) content of niobium filaments and (c) addition of titanium on the diffusion of elemental tin. (a) Cu–25 wt % Nb samples annealed at 823 K for (1) 100, (2) 500 and (3) 1500 ksec. (b) Cu–(1) 10, (2) 25 and (3) 40 wt % Nb samples annealed at 823 K for 500 ksec. (c) (1) Cu–25 wt % Nb and (2) Cu–25 wt % Nb–0.5 wt % Ti samples annealed at 823 K for 200 ksec.

became rod-like and then exhibited a sausage-like shape with increasing annealing temperature. Filaments coalesced with neighbouring filaments and also spheroidized into isolated particles at high temperatures. Fig. 8 shows the comparison of the morphology between the 10 and 40 wt % Nb samples. When the annealing temperature was relatively low, not all niobium filaments coalesced and some of the filaments spalled down by etching away the matrix in the 10 wt % Nb samples (Fig. 8a), while they coalesced with each other and no spalling was observed in the 40 wt % Nb samples (Fig. 8b). Thus the coalescence of the filaments tends to occur more in the higher niobium content samples. When the annealing temperature was high, the filaments tended to spheroidize in the low niobium content samples, as seen by comparison of Figs 8c and d.

As a measure of the coarsening, the average diameter of the filaments, d_f, was measured. d_f increased with increasing temperature, T, and time, t, for a given niobium amount of 25 wt %, as shown in Fig. 9a. The influence of titanium addition on the coarsening of the filaments was small, within the accuracy of the present work. The increase in d_f was large when the niobium content was high, as shown in Fig. 9b, because the coalescence of filaments occurred more for higher niobium contents.

3.3. Upper critical magnetic field, H_{c2}, and critical current density, J_c

3.3.1. Upper critical magnetic field, H_{c2}

Fig. 10 shows some examples of the Kramer plot [8, 9]. From the extrapolation of the $J_c^{1/2}H^{1/4}$–H curves, H_{c2} was deduced to a first approximation. Fig. 11 shows the variation of H_{c2} thus determined as a function of annealing time. The following features could be read from Fig. 11. (1) H_{c2} increased with increasing niobium content for a given annealing treatment. (2) Addition of titanium raised H_{c2}, as observed in conventional bronze-processed samples [9–13]. (3) Within the range investigated, in the case of 823 K annealing, H_{c2} increased with increasing time, while in case of 973 K annealing, it increased slightly but then decreased. (4) The change in H_{c2} for 40 wt % Nb with increasing time was small, but that for 10 wt % Nb was large. (5) The reduction in H_{c2} due to high-temperature annealing for 10 wt % Nb was large.

The increase in H_{c2} with increasing annealing time stated above in feature 3, could be attributed to the improvement of stoichiometry of Nb_3Sn as in the conventional bronze-processed samples [9, 14]. One of the reasons for the decrease in H_{c2} for long annealing times stated in feature 3 and for features 4 and 5 is presumably attributed to the change in morphology of the filaments.

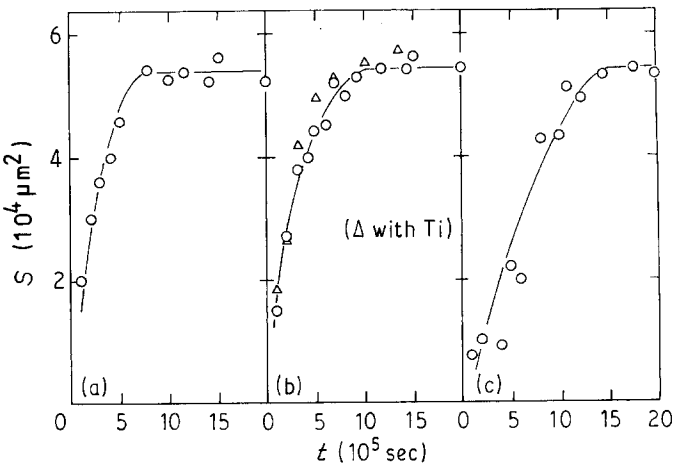

Figure 6 Increase in S with increasing annealing time, t, in the Cu– (a) 10, (b) 25 and (c) 40 wt % Nb samples annealed at 823 K, together with that in the Cu–25 wt % Nb–0.5 % Ti sample for comparison.

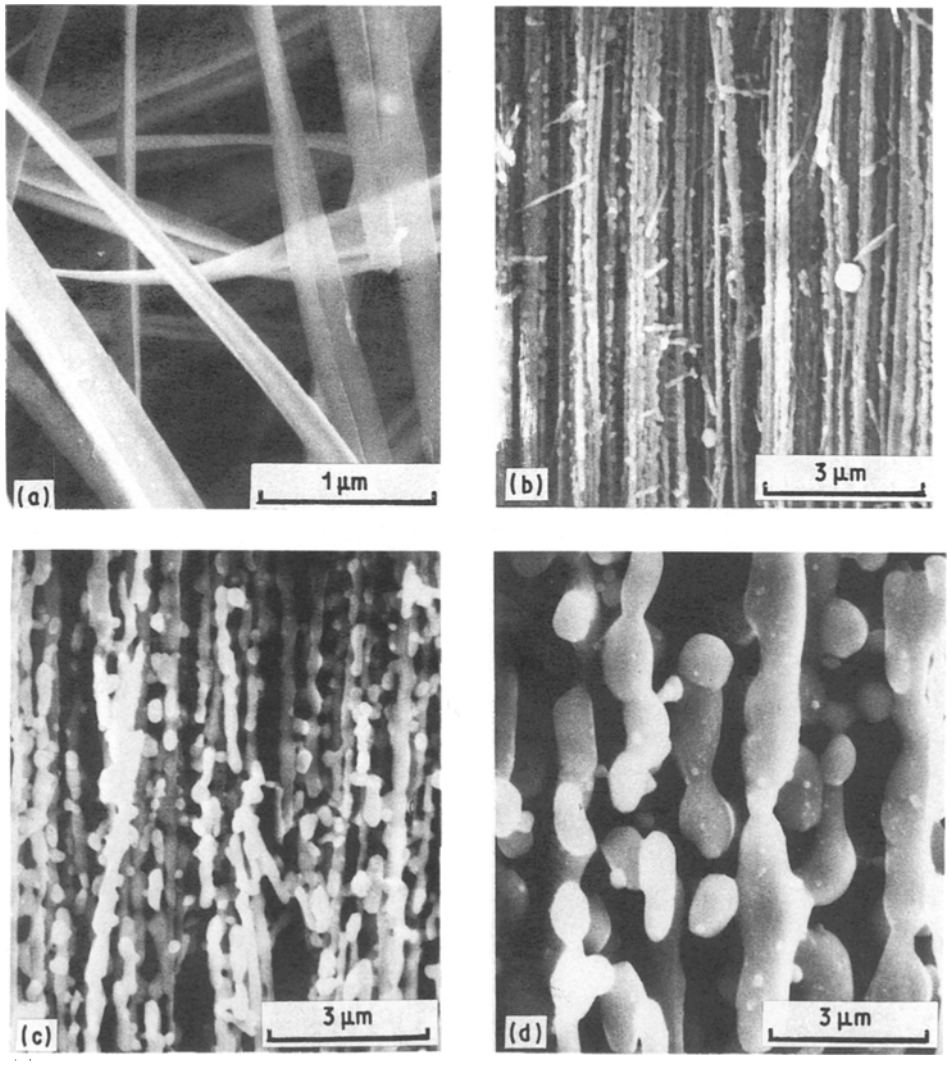

Figure 7 Change in morphology of niobium filaments in the Cu–25 wt % Nb samples due to annealing treatment. (a) As-supplied, (b) annealed at 773 K for 864 ksec, (c) annealed at 873 K for 864 ksec and (d) annealed at 1073 K for 864 ksec.

3.3.2. Critical current density, J_c

As stated in Sections 3.1. and 3.2., after annealing treatment, the diffusion of the elemental tin into the Cu–Nb core, forming Nb_3Sn, and also the change in morphology of the niobium filaments (with Nb_3Sn) occur, both of which are functions of temperature and time and amount of niobium. Thus the critical current, J_c, and upper critical magnetic field, H_{c2}, vary with varying annealing temperature and time and amount of niobium.

3.3.2.1. Influence of annealing temperature and time on critical current. Fig. 12 shows the variations of J_c at 5, 9 and 12 T as a function of annealing time for the 25 wt % Nb samples annealed at 823 and 973 K. The following features may be seen in Fig. 12. (1) J_c increased with increasing annealing time, reaching a maximum, and then decreasing at any magnetic field for both 973 and 823 K. (2) The maximum J_c was obtained around 43 and 1000 ksec for 973 and 823 K annealings, respectively. (3) The maximum values of J_c for 823 K annealing were about 1.9, 2.9 and 4.1 times higher than those for the 973 K annealing at 5, 9 and 12 T, respectively. Namely, the low-temperature annealing resulted in high J_c especially at high magnetic fields. (4) A drastic reduction in J_c for long annealing times at high temperatures (973 K) occurred.

The increase in J_c on short time annealing could be attributed to (a) the increasing amount of Nb_3Sn, as shown typically in Fig. 13 in which J_c at 5 T is plotted against the cross-sectional area, S, where the tin has diffused (Fig. 6), and (b) the increase in H_{c2} stated above.

In the case of conventionally prepared samples, the critical current density based on the cross-sectional area of Nb_3Sn itself decreases monotonically with increasing time at low applied magnetic fields due to a decrease in pin-site (grain boundaries) density for magnetic flux in Nb_3Sn, and it increases and then decreases at high applied fields due to competition with increasing H_{c2}, which acts to raise the critical current, and a decrease in pin-site density, which acts to reduce it [15]. In order to compare the current density of the present samples with that of conventional ones, the critical current density based on the cross-sectional area, S, J_c', was plotted against time, as shown in Fig. 14. If the current-controlling factors for the present samples had been the same as those for conventional ones, and the amount of Nb_3Sn had been proportional to S, the J_c' of the present work would have shown the same tendency as that of conventional samples. However, in the present work, as shown in Fig. 14, J_c' increased and then decreased with

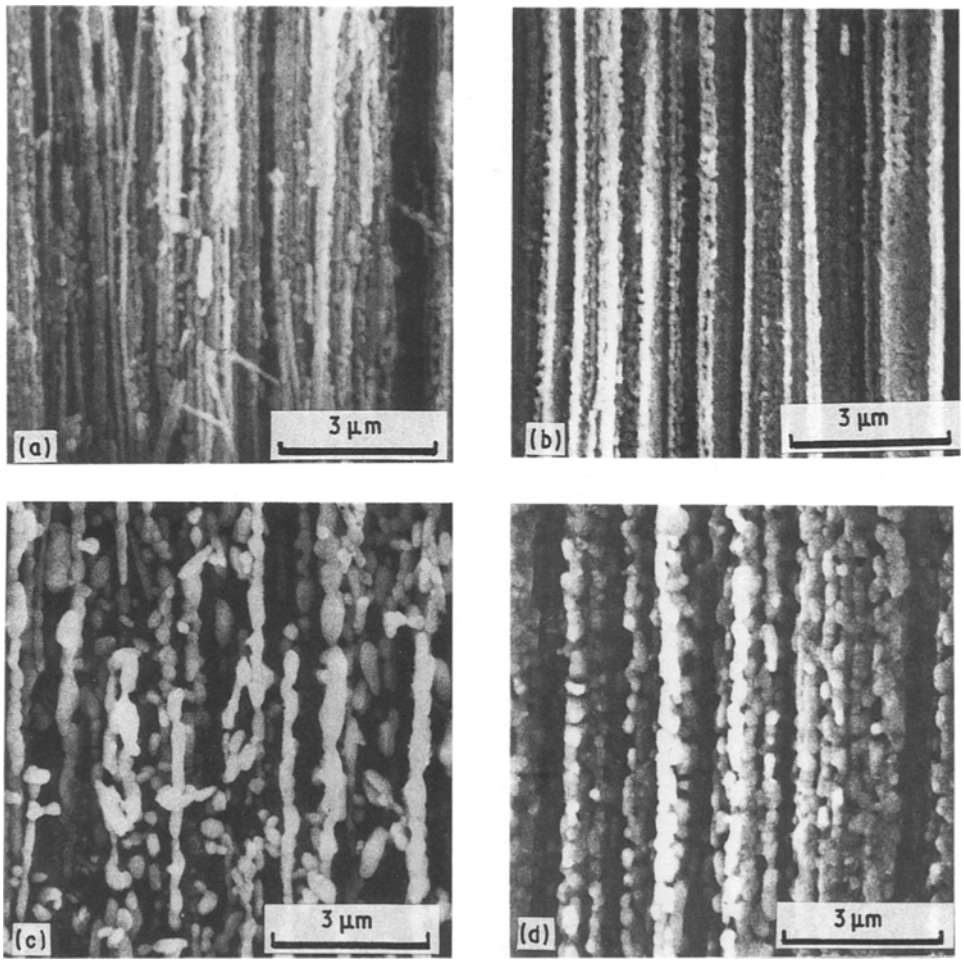

Figure 8 Appearance of the niobium filaments in the Cu–(a, c) 10 and (b, d) 40 wt % Nb samples annealed at (a, b) 823 K for 500 ksec and (c, d) 973 K for 432 ksec.

increasing time at any H. At high fields, this tendency was the same as that for conventional superconductors. However, the tendency at low fields was different in that the critical current density increased with short annealing times in the present samples, while it decreased monotonically in the conventional ones. The increase in J_c' in short-term annealing might partly be attributed to the increase in the amount of Nb_3Sn in the region where the diffusion front had passed, as indicated in Fig. 5a. Detailed study is needed for further discussion.

The reason, why the critical current density decreased when annealing time was long, may be attributed to the change in morphology of the filaments shown in Figs 7 and 8, which resulted in a reduction in the straight current path, loss of continuity of the current path, and decrease in the proximity effect. As the filaments are finite in length in the present samples, when the superconducting current in Nb_3Sn encounters

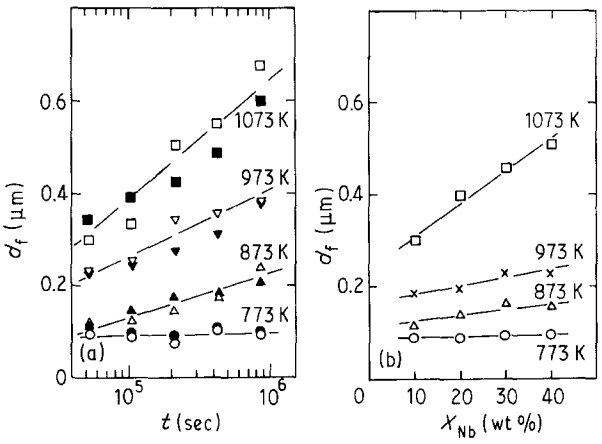

Figure 9 Measured values of d_f plotted against (a) t for the Cu–25 wt % Nb (open symbols) and Cu–25 wt % Nb–0.5 wt % Ti (closed symbols) samples annealed at 773 to 1073 K and (b) X_{Nb} for the Cu–10 to 40 wt % Nb samples annealed at 773 to 1073 K for 86.4 ksec.

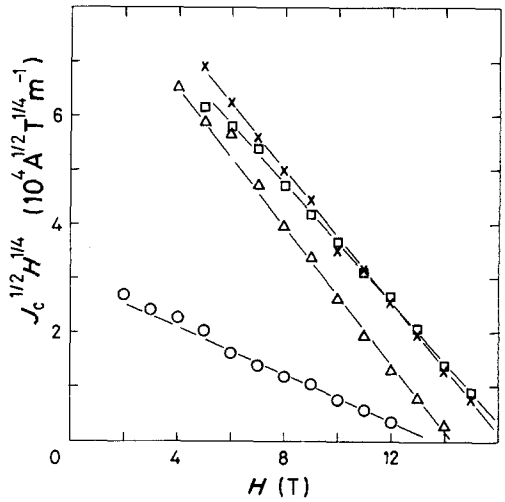

Figure 10 Examples of the Kramer plot. (○) 10 wt % Nb, (△) 25 wt % Nb, (x) 40 wt % Nb, (□) 25 wt % Nb (Ti) samples annealed at 823 K for 1000 ksec.

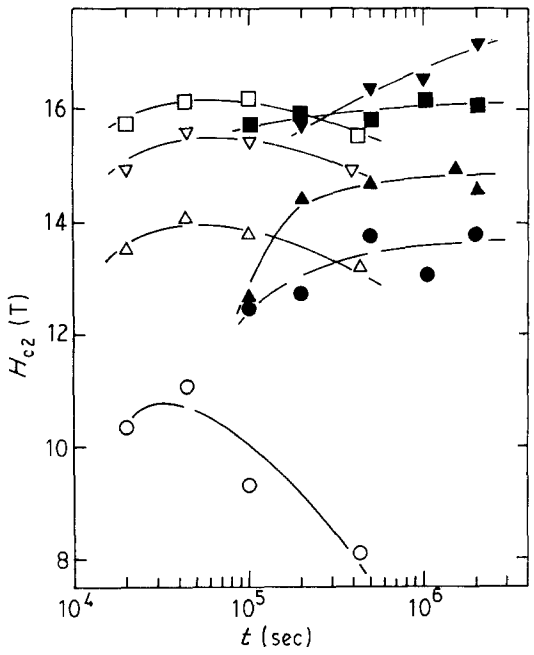

Figure 11 Measured values of H_{c2} plotted against t for all the samples employed in the present work annealed at (●, ▲, ▼, ■) 823 K and (○, △, ▽, □) 973 K. % Nb: (●, ○) 10, (▲, △) 25, (▼, ▽) 25 (Ti), (■, □) 40.

discontinuities, it leaves the present filament and moves to a neighbouring one. This proximity effect has been known to occur in the order of 0.1 μm [16, 17]. When filament spacing becomes large due to coarsening and spheriodization, the proximity effect is unable to take place, resulting in a decrease in the critical current.

3.3.2.2. Influence of niobium content on critical current. Fig. 15 shows the influence of niobium content on J_c. The following features may be seen in Fig. 15. (1) J_c increased with increasing niobium content for a given annealing treatment. (2) The difference in J_c between

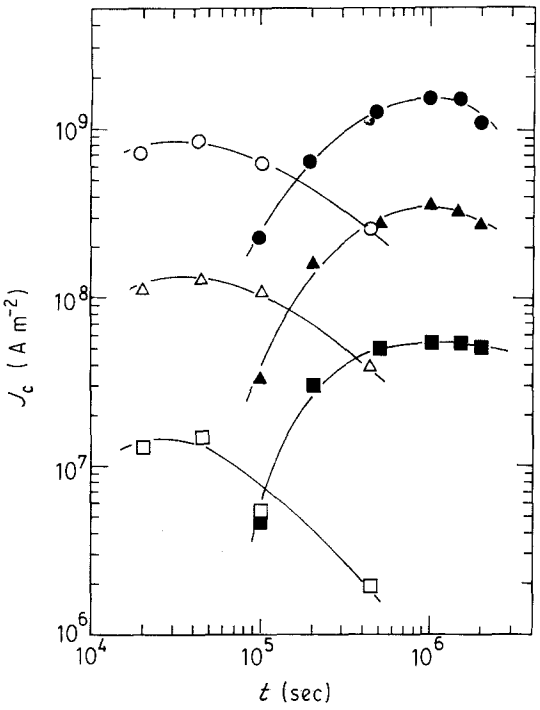

Figure 12 Variation of J_c at 5, 9 and 12 T as a function of t of the Cu–25 wt % Nb samples annealed at (●, ▲, ■) 823 and (○, △, □) 973 K. H (T): (●, ○) 5, (▲, △) 9, (■, □) 12.

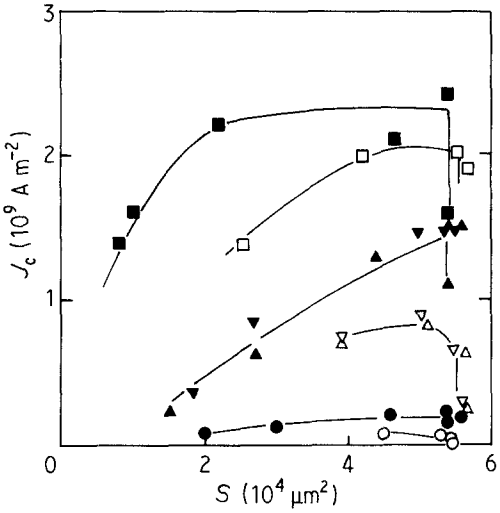

Figure 13 Variation of J_c at 5 T as a function of S, at 823 K (closed symbols) and 973 K (open symbols). X_{Nb} (%): (●, ○) 10, (▲, △) 25, (▼, ▽) 25 (Ti), (■, □) 40.

low and high niobium content samples increased at high magnetic fields. For instance, in the case of samples annealed at 823 K for 500 ksec, J_c at 12 T for 40 wt % Nb was about 30 times higher than that for 10 wt % Nb, while J_c at 5 T for the former sample was only about 10 times higher than that for the latter sample. (3) The difference in J_c between low and high niobium content samples became large for high-temperature annealing. For instance, comparing J_c at 5 T between the 10 and 40 wt % Nb samples, the J_c value for 40 wt % Nb was about 10 times higher than that for 10 wt % Nb in the case of 823 K annealing, while the former was about 100 times higher than the latter in the case of 973 K annealing.

One of the reasons why high niobium content samples showed high J_c could be attributed to the high amount of Nb_3Sn formed. However, this reason was insufficient to explain all the experimental results. For instance, when J_c at 5 T was plotted against the product S and X_{Nb}, which is proportional to the amount of Nb_3Sn formed in very rough estimation, J_c for high X_{Nb} was still higher than that for low X_{Nb}, as shown in Fig. 16, suggesting that J_c for high niobium contents was higher than that predicted based only on the amount of Nb_3Sn formed.

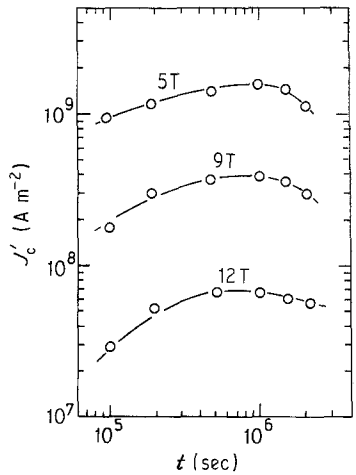

Figure 14 Variation of J_c' at 5, 9 and 12 T as a function of t of the Cu–25 wt % Nb samples annealed at 823 K.

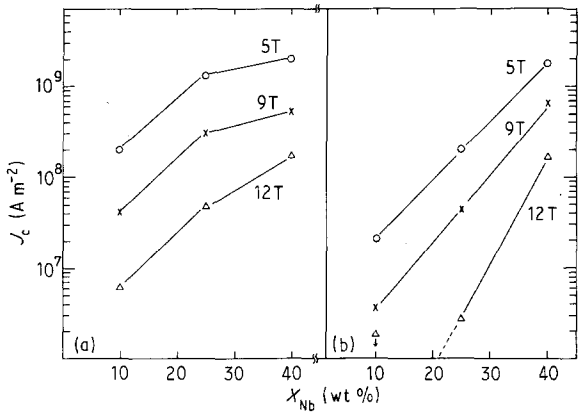

Figure 15 Measured values of J_c at 5, 9 and 12 T plotted against X_{Nb} of the samples annealed at (a) 823 K for 500 ksec and (b) 973 K for 432 ksec.

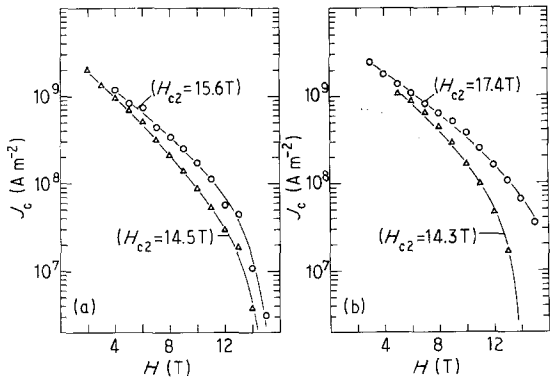

Figure 17 Comparison of J_c of (○) titanium-doped Cu–25 wt % Nb samples with that of (△) undoped ones annealed at 823 K for (a) 200 and (b) 2000 ksec.

In the present samples, the filaments in low niobium content samples showed more spheroidization than those in high niobium content samples, as shown in Fig. 8. This means that higher continuity for current path could be retained in the high niobium content samples than in the low niobium content ones. Also, as the inter-filament spacing in the high niobium content samples was essentially narrower than that in the low niobium content samples the effective proximity effect could arise to a greater degree in the high niobium content samples. These may be the reasons for the high J_c with high niobium contents.

3.3.2.3. Influence of titanium addition on critical current. Fig. 17 shows the influence of titanium addition on the critical current. The addition of titanium raised J_c effectively, as in conventional superconductors. The reason for this could be attributed to (a) an increase in the amount of Nb_3Sn, as shown in Fig. 5c, and (b) an increase in H_{c2}, as shown already in Fig. 11.

4. Conclusions

1. High amounts of tin plated on the samples enhanced the diffusion of elemental tin. The critical current increased with increasing tin thickness but the increase became sluggish at high tin contents.

2. The niobium filaments with initially ribbon-like shape became rod-like and then sausage-like after annealing treatments. This morphological change acted to reduce the superconducting current capacity. When the amount of niobium was low, the filaments spheroidized when annealed at high temperatures for long times, resulting in a serious reduction in the critical current and the upper critical magnetic field.

3. High niobium contents led to high critical currents and high upper critical magnetic fields due to the retainment of continuity of the filaments after annealing, the effective proximity effect and a high amount of Nb_3Sn formed in comparison with low niobium contents.

4. Titanium addition raised the upper critical magnetic field, resulting in an improvement in the critical current, especially at high magnetic fields.

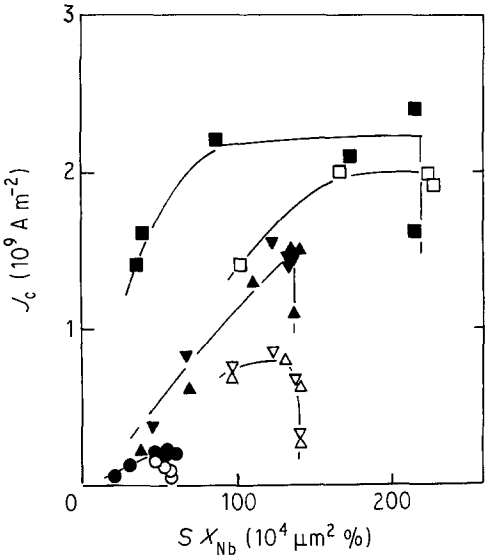

Figure 16 Measured values of J_c at 5 T plotted against SX_{Nb}. T: 823 K (closed symbols) and 973 K (open symbols). X_{Nb} (%): (●, ○) 10, (▲, △) 25, (▼, ▽) 25 (Ti), (■, □) 40.

Acknowledgements

The authors thank Professors T. Muto, K. Watanabe, K. Noto and A. Hoshi, Messrs K. Kudo, K. Sai and Y. Ishikawa, High Field Laboratory for Superconducting Materials, Tohoku University, for their help in the critical current measurements, and Messrs T. Uneaki and I. Nakagawa for their help in the EPMA and SEM studies. They also thank the Ministry of Education, Science and Culture of Japan for the grant-in-aid for energy research (no. 63055026).

References

1. R. ROBEGE, in "Superconductor Materials Science", edited by S. Foner and B. B. Schwarz (Plenum, New York, 1981) p. 258.
2. J. BERK, J. P. HARBISON and J. L. BELL, *J. Appl. Phys.* **49** (1978) 6031.
3. K. R. KARSEK and J. BEVK, *Scripta Metall.* **13** (1979) 259.
4. B. A. ZEITLIN, G. M. OZERYANSKY and K. HEMACHALAM, *IEEE Trans. Mag.* **MAG-21** (1985) 293.
5. R. ROBERGE, S. FONER, E. J. MCNIFF Jr, B. B. SCHWARZ and J. L. FIHEY, **MAG-15** (1979) 687.
6. J. W. EKIN, *ibid.* **MAG-15** (1979) 197.
7. A. NAGATA, K. HAYASHI, T. HANANO and O. IZUNI, *Trans. Jpn Inst. Met.* **26** (1985) 663.
8. E. J. KRAMER, *J. Appl. Phys.* **44** (1973) 1360.
9. M. SUENAGA, in "Superconductor Materials Science", edited by S. Foner and B. B. Schwarz, (Plenum, New York, 1981) p. 201.

10. M. SUENAGA, W. B. SAMPSON and T. S. LUHMAN, *IEEE Trans. Mag.* **MAG-17** (1981) 646.
11. K. TACHIKAWA, T. ASANO and T. TAKEUCHI, *Appl. Phys. Lett.* **39** (1981) 766.
12. K. TACHIKAWA, H. SEKINE and Y. IIJIMA, *J. Appl. Phys.* **53** (1982) 5534.
13. K. OSAMURA, S. OCHIAI, S. KONDO, M. NAMATAME and M. SOSAKI, *J. Mater. Sci.* **21** (1986) 1509.
14. S. OCHIAI and K. OSAMURA, *Acta Metall.* **34** (1986) 2425.
15. *Idem, ibid.* **35** (1987) 1433.
16. H. MEISSNER, *Phys. Rev.* **117** (1960) 672.
17. C. J. KIRCHER, *ibid.* **168** (1968) 437.

Received 6 April
and accepted 28 September 1989